Cosmic microwave anisotropies from topological defects in an open universe

Ue-Li Pen and David N. Spergel
Princeton University Observatory, Princeton, New Jersey 08544
(Received 30 August 1994)

We present a general formalism for computing cosmic background radiation (CBR) and density fluctuations in open models with stiff sources. We decompose both the metric fluctuations and the fluctuations in the stress-energy tensor into scalar, vector, and tensor modes. We find analytic Green's functions for the linearized Einstein equations in the presence of stiff sources and use this formalism to estimate the amplitude and harmonic spectrum of microwave background fluctuations produced by topological defects in an open universe. Unlike inflationary models that predict a flat universe and a spectrum of CBR fluctuations that are enhanced at large angular scales, defect models predict that CBR fluctuations are suppressed on angular scales larger than that subtended by the curvature scale. In an $\Omega = 0.2 - 0.4$ universe, these models, when normalized to the amplitude of CBR fluctuations observed by COBE, require a moderate bias factor, 2–3, to be compatible with the observed fluctuations in galaxy counts. In these models, accurate predictions can be made which are testable through CBR experiments in the near future. A CBR measurement of Ω would then be possible, up to the limit imposed by cosmic variance. We discuss some of the philosophical implications of an open model and propose a solution to the flatness problem.

PACS number(s): 98.80.Cq, 11.27.+d

I. INTRODUCTION

In recent years, most theoretical work in cosmology has assumed that the universe is flat and matter dominated. This assumption is nearly inevitable in inflationary scenarios that predict that Ω should be close to unity. However, defect models make no such predictions for the density of the universe.

There is a host of astronomical evidence that suggests that the universe may be open. White *et al.* [1] argues that x-ray observations of clusters imply that at least 20% of their mass is baryonic. When combined with standard hot big-bang estimates of the baryon density [2], $\Omega_b h^2 \simeq 0.015$, this implies that the total density in nonrelativistic matter is much less than unity. Observations of galaxy random velocities [3] find that $\sigma_8 = 317$ km/s, a factor of 4 below the predictions of Cosmic Background Explorer (COBE) normalized flat scale-invariant cosmologies. The matter density inferred from comparisons between the galaxy correlation function in redshift and real space is also much smaller than unity and is compatible with $\Omega \sim 0.3$ [4].

Over the past decade, observational cosmologists have devoted much effort to measuring the spectrum of density fluctuations and have found significant evidence for more large-scale structure than predicted in flat universe models. As the predicted spectrum of density fluctuations is peaked on the physical scale corresponding to the horizon size at matter-radiation equality, $32/\Omega h^2$ Mpc, models with $\Omega = 1$ predict less large-scale power than low Ω models. For example, the standard cold dark matter (CDM) model underpredicts the ratio of galaxy fluctuations observed on the $30/h$ Mpc scale in the 1.2 Jy survey to galaxy fluctuations inferred on the $1/h$ Mpc scale in the same survey by nearly a factor of 5. On the other hand, CDM models with $\Omega h \sim 0.2$ are remarkably successful at fitting observations of large-scale structure [5].

In a flat universe, topological defect models also fail to produce the observed large-scale structure. Albrecht and Stebbins [6] found that the predicted spectrum of density fluctuations in a cosmic string model is peaked on the string coherence scale, which is even smaller than the horizon size. Because of this lack of large-scale power, they concluded that a string-seeded CDM model was not compatible with the observed large-scale structure and failed more dramatically than the inflationary scenarios. Pen, Spergel, and Turok (PST) [7] explored global defects such as global strings, monopoles, texture, and nontopological textures. The rich dynamics of these non-Gaussian isocurvature fluctuations have provided a challenge and stimulus to the field of cosmological perturbation theory [8], where the gauge invariant formalism has been refined for that purpose [9]. Microwave background predictions have recently also been calculated by Borrill *et al.* [10] and Bennett and Rhie [11].

While monopoles, texture, and nontopological textures all predict a power spectrum of density fluctuations with more large-scale power than the cosmic string model, these models still fail to produce the observed level of galaxy fluctuations by nearly an order of magnitude on the $20/h$ Mpc scale. This failure is due to the defect coherence scale at equality being too small. As this scale is proportional to Ωh^2, this problem will be alleviated in a low Ω universe.

In the excitement following the announcement [12,13] that COBE has detected thermal fluctuations in the cosmic microwave background (CBR), many cosmologists declared that the detection was evidence for a flat universe and the inflationary scenario. This, however, need not be the only interpretation of the COBE results. The

two-year COBE results [14] are also consistent with open universe models with either adiabatic density fluctuations [15,16] or equation-of-state density fluctuations [17].

Inflationary scenarios predict either a scale-invariant spectrum of CBR fluctuations or a spectrum of fluctuations that has more power on large angular scales [18]. In models with significant gravity wave contribution and in power law inflationary models [19], the low multipole fluctuations are enhanced relative to fluctuations on small angular scales. Inflationary models with cosmological constant [20] also predict enhanced contributions on large angular scales. On the other hand, analysis of COBE's two-year data set [22,14] suggest that the low multipoles are not enhanced but suppressed relative to the fluctuations on smaller angular scales. While there is still a significant statistical uncertainty in the two-year COBE data, the Tenerife CBR observations [23] and the FIRS results [24] also hint that the slope of CBR fluctuations may be steeper than that predicted in any inflationary models. This steep CBR fluctuation spectrum is one of the predictions of open universe models [17]. If the suppression of the low multipoles is still seen in the four-year data, then the COBE data may turn out to be incompatible with most inflationary scenarios.

If the universe is open, then topological defect models are particularly attractive. The basic concept of inflation lies in solving the monopole and horizon problems through an extended de Sitter phase. As other authors [25] have pointed out, the curvature of spacelike section in a de Sitter and also an empty universe depends on the choice of coordinate systems, and could be either flat or hyperbolic. The prime reason for considering a flat universe a generic prediction of inflation is the presence of the flatness problem. In this paper we will propose a solution along the lines of Linde, by using the weak anthropic principle as a selection effect. It hinges on the huge photon to baryon ratio (approximately 10^{10}), and gives a natural scale to the problem. The weakest point of inflation has been the fine tuning of parameters required to generate the observed potential fluctuations. So even within the framework of inflation, topological defects may still be desirable as they explain this fine tuning more naturally.

But quite independently of the existence of inflation, if we are left to find another route for explaining the large-scale homogeneity of the universe, it would be most natural to assume that the universe started with smooth initial conditions and that causal physics generated density fluctuations. Spergel [17] presents analytical arguments that suggested that defect models are likely to be compatible with observations of large-scale structure in an open universe. In this paper, our numerical calculations support these arguments and suggest that these models merit careful consideration.

This article builds upon the analytical and numerical techniques presented in PST. In PST, we attempted to quantitatively compare the predictions to topological defect models in a flat universe to the COBE observations and the observations of large-scale structure. This paper extends our approach to an open universe. Our CBR calculations make no assumptions about the nature of the dark matter. However, when we compare the COBE normalized theories to the observed large-scale structure, we assume that the universe is dominated by cold dark matter.

In this paper, we estimate the amplitude of CBR fluctuations generated by various topological defect scenarios. Because of ease of computation, we focus on the texture models, for which analytic and semianalytic methods have also been applied in flat universes [26,27]. While we have deferred the challenge of evolving a string network in a hyperbolic universe, we believe that qualitatively the results of this paper can be extrapolated to other defect models. In Sec. II, we extend the analytical formalism that we developed in PST to open universe models. In Appendix B, we also extend the formalism to vacuum-dominated models. In Appendix C we extend formalism to closed models. In Sec. III, we describe our numerical algorithms for computing defect evolution. In Sec. IV, we present our numerical results and emphasize the characteristic CBR signature of defects in open universe models and then we discuss the predictions of the COBE-normalized open universe models for large-scale structure. In Sec. V, we discuss philosophical motivations for open universes. In Sec. VI, we sum up.

II. CBR FLUCTUATIONS IN AN OPEN UNIVERSE

In this section, we modify the formalism developed in PST so that we can calculate the amplitude of CBR fluctuations produced in an open universe.

The assumptions entering in the calculations are the weak field limit for gravity, which allows us to treat gravitational perturbations in linearized form. The quantum field is evolved as a classical field, as it is a boson field with large occupation number. An additional assumption is the stiffness of the source term, that gravity does not affect the evolution of the defects. This is certainly justified for global defects, which dissipate their energy into Goldstone modes. In the case of gauged cosmic strings one needs to account for their energy dissipation in gravity waves. The defect field is governed by the nonlinear σ model, which is a highly nonlinear evolution equation. While certain scaling laws can be computed in a flat space time [28], this is not possible in the transition regime between matter and curvature domination. The field correlation length cannot be accurately specified, and most analytic approaches are no longer applicable. Thus one needs to simulate the field evolution numerically, and measure these quantities.

The gravity is, however, still linear, and we will show below how to solve that problem in an open universe once we are given the source terms. They are still straightforward integrals over the energy momentum tensor with certain Green's functions.

In PST, we decomposed variations in the source stress energy tensor and fluctuations in the metric into scalar, vector, and tensor components. Variations in the trace of the spatial stress energy tensor generate growing density modes that can form galaxies. The traceless (also

called anisotropic) scalar source term, the vector source term, and the tensor source terms do not generate growing density modes; however, they do source decaying metric fluctuations that produce CBR fluctuations. We have reexamined our flat universe simulations and found that the CBR fluctuations generated by the scalar modes are the dominant source of fluctuations: the scalar growing mode term alone accounts for 70% of the CBR fluctuations.

The decomposition into scalar, vector, and tensor modes is a nonlocal calculation that is numerically challenging in an open universe. In order to evaluate the viability of defect models in an open universe, we will focus on only the contributions of the growing scalar mode in this calculation. In an open universe, we expect that the vector and tensor modes are even less important than in a flat universe as they are suppressed relative to the scalar modes by powers of (v/c), where v is the defect velocity. In an open universe, the rapid expansion of the universe slows the defect velocities. Because of our ignoring the anisotropic stress, vector and tensor modes, the amplitude of CBR fluctuations calculated in this paper should be multiplied by a factor between 1–1.2.

In PST, we showed that the variations in the trace of the spatial stress, Θ, source variations in the scalar piece of the metric [PST 46]:

$$\ddot{h}^- + 2\frac{\dot{a}}{a}h^- = -8\pi G\Theta \equiv S \ . \tag{1}$$

These metric fluctuations contribute to the Sachs-Wolfe integral:

$$\left(\frac{\delta T}{T}\right) = -\frac{1}{2}\int_i^f d\eta \dot{K}[x(\eta),\eta] \ , \tag{2}$$

where

$$K = \left(\frac{h^-}{3} - \mathcal{J}\right) \tag{3}$$

[PST 50] and

$$\dot{\mathcal{J}} + 2\frac{\dot{a}}{a}\mathcal{J} = -\frac{1}{3}h^- \tag{4}$$

[PST 49]. Here, a is expansion factor and dot denotes derivative with respect to the conformal time η. For more details on the notation and conventions, see Appendix A. In the notation of PST, $J = k^2\mathcal{J}$.

After a little algebra, Eqs. (1), (3), and (4) can be combined to yield an equation for the scalar stress contribution to CBR fluctuations:

$$\dot{K}(x,\eta) = \int_0^\eta d\tilde{\eta} S(x,\tilde{\eta}) \left[\frac{a(\tilde{\eta})^2}{a(\eta)^2} - \frac{\dot{a}(\eta)}{a(\eta)}a(\tilde{\eta})^2 E(\eta,\tilde{\eta}) - \left(\frac{\ddot{a}(\eta)}{a(\eta)} - 3\frac{\dot{a}(\eta)}{a(\eta)^2}\right)\frac{a(\tilde{\eta})^2}{a(\eta)^2}H(\eta,\tilde{\eta})\right] \ , \tag{5}$$

where

$$E(\eta,\tilde{\eta}) = \int_{\tilde{\eta}}^\eta \frac{d\bar{\eta}}{a(\bar{\eta})^2} \tag{6}$$

and

$$H(\eta,\tilde{\eta}) = \int_{\tilde{\eta}}^\eta a(\bar{\eta})^2 d\bar{\eta}\int_{\tilde{\eta}}^{\bar{\eta}} \frac{d\eta'}{a(\eta')^2} \ . \tag{7}$$

Note that E can also be used to relate the vector stress energy source term to the vector metric fluctuations term [PST 47] and to evolve the decaying scalar metric fluctuations [PST 49].

In a flat matter-dominated universe, $a(\eta) = \eta^2$, thus, $E(\eta,\tilde{\eta}) = 1/3\eta^3 - 1/3\tilde{\eta}^3$ and $H(\eta,\tilde{\eta}) = \eta^5/15\tilde{\eta}^3 - \eta^2/6 + \tilde{\eta}^2/10$. Combining these results with Eq. (5) yields

$$\dot{K}(x,\eta) = \int_0^\eta d\tilde{\eta} S(x,\tilde{\eta})\left(\frac{\tilde{\eta}^6}{\eta^6}\right) \ . \tag{8}$$

This simple result is due to the simple form of $a(\eta)$.

In an open matter-dominated universe, the expansion factor has a more complicated form:

$$a(\eta) = \frac{\Omega_0}{-\mathcal{K}}\left[\cosh(\sqrt{-\mathcal{K}}\eta) - 1\right] \ , \tag{9}$$

where Ω_0 is the density in matter today and $\mathcal{K}$ is the curvature scale. For the rest of the paper, we set $\mathcal{K} = -1$ and use it as the physical length scale in the calculation. Note that for small η, Eq. (9) approaches the flat space form. Combining Eq. (9) with Eqs. (6) and (7) yields

$$E(\eta,\tilde{\eta}) = \frac{\dot{a}(\bar{\eta})}{3a(\bar{\eta})^2}(1 - a(\bar{\eta}))\Big|_{\bar{\eta}=\eta}^{\tilde{\eta}} \tag{10}$$

and

$$H(\eta,\tilde{\eta}) = \frac{1}{\tilde{a}} - \frac{5}{6} + \frac{a^2}{6} - \frac{a}{3} + \frac{\dot{a}(\tilde{\eta})\,[1-\tilde{a}]}{6\tilde{a}^2} \times [\dot{a}(\eta)(a-3) + 3(\eta - \tilde{\eta})] \ , \tag{11}$$

where $\tilde{a} = a(\tilde{\eta})$ and $a = a(\eta)$. Equations (5), (10), and (11) can now be combined to yield

$$\dot{K}(x,\eta) = \int_0^\eta d\tilde{\eta} S(x,\tilde{\eta})\left\{\frac{\tilde{a}^2}{a^2}\left[1 + \frac{2 - a - a^2}{3} + \left(\frac{5}{a} + 2\right) \times \left(\frac{a^2}{6} - \frac{a}{3} - \frac{5}{6}\right)\right] + \tilde{a}(1-\tilde{a})\left[\frac{-\dot{a}}{3a} + \left(\frac{5}{a} + 2\right)\frac{\dot{a}(a-3) + 3\eta}{6a^2}\right] + \left[\tilde{a} - \dot{\tilde{a}}(1-\tilde{a})\tilde{\eta}\right]\frac{5 + 2a}{a^3}\right\}. \tag{12}$$

In the limit of small η, Eq. (12) reduces to Eq. (8).

The vector modes still allow a simple integral, for which we have

$$\dot{h}_i^V = \frac{16\pi G}{a^2}\int a(\eta')^2\Theta_i^V d\eta'. \tag{13}$$

Tensor modes, on the other hand, propagate and require two Green's functions to express. As in [PST 54], we write

$$h_{ij}^T = 16\pi G \int \left[\frac{G_1(\eta')G_2(\eta) - G_2(\eta')G_1(\eta)}{W(\eta')} \Theta_{ij}^T(\eta) \right] d\eta' \ , \tag{14}$$

where now the Green's functions are

$$\begin{aligned} G_1 &= \frac{\cos(k\eta)}{a} - \frac{\sin(k\eta)\dot{a}}{2a^2} \ , \\ G_2 &= \frac{\cos(k\eta)\dot{a}}{2a^2} + \frac{\sin(k\eta)}{a} \ , \\ W &= G_1\dot{G}_2 - G_2\dot{G}_1 \ . \end{aligned} \tag{15}$$

We have assumed a decomposition in terms of eigenfunctions of the Laplace-Beltrami operator ∇^2, which in our framework will be the sum of two sine frequencies and one Bessel function index. Note that the tensor mode Green's function in Eq. (15) are valid for open, flat, and closed models.

In the next section, we present our numerical algorithms for evolving the defect field to compute $S(x, \tilde{\eta})$, for integrating Eq. (12) to compute the metric fluctuations, and for following photon trajectories to integrate Eq. (2).

III. NUMERICAL IMPLEMENTATION

In this section we describe the numerical implementation issues. The original program is freely available by anonymous *ftp* from `astro.princeton.edu` in /upen/StiffSources/openuniverse. It is written in standard C++ and C, and should compile and execute on any machine with these compilers. It is optimized to execute very efficiently on the convex vector architecture. In fact, simulations are always limited by memory, because the volume of a hyperbolic universe is exponentially large, so the computation time scales as $O(N\log(N))$ where N is the memory requirement.

The basic strategy will be to apply the mode decomposition from PST. In order to work in an open universe, many changes need to be applied which are described below.

A. Grid

The very first obstacle is the formulation of a regular lattice to discretize a hyperbolic manifold. The requirements are (1) it must have constant volume per lattice element, (2) appear locally Euclidean, (3) be easily mapped onto the serial storage of a computer, and (4) allow the Laplacian to be easily invertible.

For this purpose the Poincaré metric provides a very nice tiling, which retains many of the regularities of a flat space Cartesian lattice. The spatial metric is given by the line element

$$ds^2 = \frac{dx^2 + dy^2 + dw^2}{w^2}. \tag{16}$$

With a change of variables $z = \ln(w)$, we satisfy all the requirements stated above. On small scales, it is explicitly Euclidean, which simplifies the implementation of the differential operators. This metric maps onto the more familiar Friedmann coordinates (χ, θ, ϕ) through the change of variables

$$\begin{aligned} x &= \frac{\cos(\phi)\sinh(\chi)}{\cosh(\eta - \chi)} \ , \\ y &= \frac{\sin(\phi)\sinh(\chi)}{\cosh(\eta - \chi)} \ , \\ z &= \frac{\cosh(\eta)}{\cosh(\eta - \chi)} \ , \\ \cos(\theta) &= \tanh(\eta). \end{aligned} \tag{17}$$

The mapping onto the Friedmann coordinates is shown in Fig. 1. The inverse mapping is displayed in Fig. 2. The salient features of this metric are the explicit translational symmetry along all three dimensions, and the rotational symmetry about the z axis. The only explicit numeric anisotropy occurs for rotations in the x-z and y-z planes. This effect is easily tested for in the simulations by checking the alignment of the quadrupole with the coordinate grid.

B. Technical issues

For simplicity, we will work in units where $\Delta t = \Delta z = 1$. The horizontal discretizations $\exp(-z)\Delta x$, $\exp(-z)\Delta y$ are adjusted to be as close to unity as possible, while still satisfying the periodicity constraints. In these units our free discretization pa-

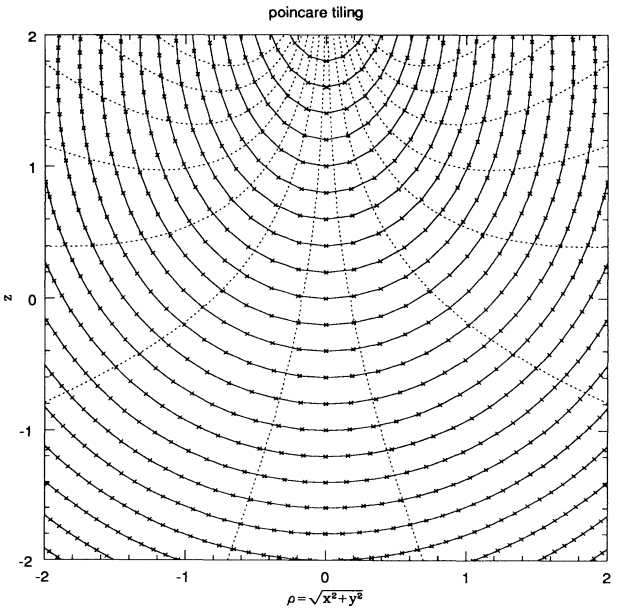

FIG. 1. The solid lines are the equispaced surfaces (called tiers) of constant z. The dotted lines are geodesics of constant x. The periodicity boundary is selected along one of these curves. The crosses indicate the location of our numerical grid points, which are regular and evenly spaced in the Poincaré metric.

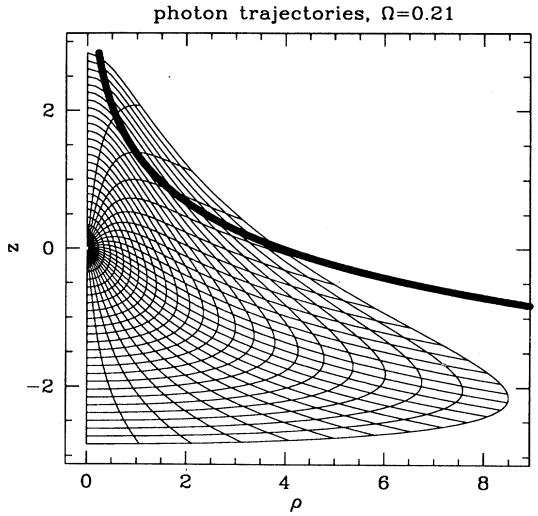

FIG. 2. This figure depicts various photon geodesics in the Poincaré frame. The axes are in units of constant distance, so $\rho = \exp(-z)(x^2+y^2)$ and $z = \ln(w)$. The heavy line is the fiducial geodesic along which our grid is periodic. The radial lines show the trajectory traversed by photons. The concentric lines are circles of constant distance from the origin, i.e., spheres in the Poincaré frame.

rameters are the curvature radius R, the mesh height H and the periodicity length L at $z = 0$. We choose $-H/2 < z < H/2$. We divide the computational grids into tiers T_i at constant z_i, each of which is a square matrix. We need to subdivide T_i into an integral number of lattice points, for which we calculate the integer such that the area bounded by each lattice cell most closely approximates unit volume. Since the T_i are represented by regular matrices, all parallelizations and vectorizations are performed at this level. The tier concept is then implemented as a C++ class. The key operation is the projection (interpolation) of one tier into the geometry of its neighboring tier above or below,

$$P_+ : T_i \longrightarrow T_{i+1}, \quad P_- : T_i \longrightarrow T_{i-1}. \tag{18}$$

In order for the discretization errors to be small, one needs to have several grid cells per curvature length. Another limiting constraint is the scaling behavior. In flat space, many defects achieve a scaling solution where the energy density is proportional to $1/a^3$. We require the numerical solution to achieve such a scaling law before the horizon size grows to the curvature scale.

C. Mode decomposition

Our basic tool is the fast Fourier transform (FFT). Since the grid is periodic in x and y, we can write any function ϕ as a sum of Fourier components,

$$\phi(x,y,z) = \sum_{n,m} \exp\left[\frac{2i\pi(nx+my)}{L}\right] \phi(n,m,z). \tag{19}$$

In order to retain discrete orthogonality, the numerical grid points must be all aligned at the phase origin $x = y = 0$. Then we simply keep a different number of Fourier modes at each z. The Laplacian becomes a second order differential operator for z,

$$\nabla^2\phi = -\frac{4\pi^2(n^2+m^2)}{L^2}\phi + e^{-z}\frac{\partial}{\partial z}\left(e^z\frac{\partial\phi}{\partial z}\right), \tag{20}$$

which we integrate to second order accuracy.

In terms of the discretized variables,

$$\nabla^2\phi = 2\frac{\cos(\pi n/n_k)+\cos(\pi m/m_k)-2}{L}\phi + \frac{\exp(-z_k)\left[\exp(z_{k+1/2})(\phi_{k+1}-\phi_k) - \exp(z_{k+1/2})(\phi_k-\phi_{k-1})\right]}{\Delta z^2}. \tag{21}$$

Note that the maximal mode n, m depends on the level of the tier. In the case that the tier above does not contain a corresponding mode, we use a zero boundary condition in Fourier space. Equation (21) is a tridiagonal system which can be solved in linear time.

Some care needs to be taken with the boundary conditions. One can easily violate causality from the nonlocal inversion of the Poisson operator. We thus need a boundary condition consistent with causality. A simple approach would be to set the boundary at the edges of the computational domain, z_u, z_l to zero.

In analogy with electromagnetism, the zero boundary conditions can be physically interpreted as a distribution of surface charges which cancel the desired fields. They cause waves to be reflected at the boundaries, so that the gravitational field boundary conditions become consistent with the field evolution.

The moving boundary condition can source scalar field and gravity waves, but since these only travel at the speed of light, a buffer zone will prevent them from affecting the photon cone in the calculations.

D. Field evolution

We implement a nonlinear σ model following the same approach as used in PST. The equation of motion for the continuum field reads

$$\frac{1}{a^2}\partial_\eta a^2 \partial_\eta \phi = \nabla^2\phi + \lambda\phi\,, \tag{22}$$

where λ is a Lagrange multiplier which must be chosen to satisfy the constraint $\phi^2 = 1$. The time discretization has two degrees of freedom, corresponding to the initial values of ϕ and $\dot{\phi}$, which we represent through the field

configuration at two consecutive time steps. We proceed in two steps. First we calculate the Laplacian. Then we advance the field in the direction of the Laplacian subject to the constraints of the nonlinear σ model. We treat the two issues in turn.

In the Poincaré metric, the Laplacian is expressed as

$$\nabla^2\phi = \exp\left(-\frac{2z}{R}\right)(\phi_{,xx}+\phi_{,yy}) + \exp\left(-\frac{z}{R}\right)\partial_z \exp\left(\frac{z}{R}\right)\phi_{,z}. \quad (23)$$

The first two terms are trivial to calculate with the standard central difference formula. With the help of the projection operators P_+, P_- we can easily evaluate the vertical derivative

$$\exp\left(-\frac{z_k}{R}\right)\left[\exp\left(\frac{z_{k+1/2}}{R}\right)(P_-\phi_{k+1}-\phi_k) - \exp\left(\frac{z_{k-1/2}}{R}\right)(\phi_k - P_+\phi_{k-1})\right]. \quad (24)$$

Along the x, y axes we can simply use periodic boundary conditions. At the top of the grid $z = H/2$ we simply extend our grid upward, which costs very little in computational effort or memory because very little volume is enclosed in that region. The bottom boundary needs to be treated more carefully. We choose a safety buffer zone of a few grid cells below the last grid point that is traversed by photons.

E. Implementation

For texture models, there is reason to believe that the primary contribution comes from the spatial trace of the energy momentum tensor,

$$\Theta = \sum_{i=1}^{3} T_i^i. \quad (25)$$

In flat and empty space, the exact texture solution generates an energy momentum tensor which is such a pure trace. As we describe below, the problem is isomorphic to such a flat problem in both the early and late time limits. The main contribution thus arises from the trace. In our current implementation, we have chosen the approximation to only retain the trace part. For other defects, especially the cosmic strings, other components of the energy momentum tensor are expected to play a dominant role and one needs to implement the full mode decomposition described above.

The simulations are constrained on several ends. We need a fair number of grid cells per curvature radius in order to achieve an accurate flat scaling density for the field before the numerical horizon size becomes comparable with the curvature scale. A violation of this constraint would cause the simulation to enter the curvature transition with an incorrect energy density, which would appear as a systematic subsequent error. In practice this corresponds to about eight grid cells per curvature radius.

With the 2 Gigabytes of memory on our convex C3440 we can run simulations down to $\Omega = 0.2$, which take about 4 hours of (wall clock) execution time.

F. Tests of the code

The two extreme limits of the parameter space have exact solutions. When $\Omega = 1$, we have an expanding flat space and we can test the exact scaling solution for a single unwinding texture as we did in the flat space calculations [7]. The other limit $\Omega = 0$ is an empty universe, which is nothing more then Minkowski space. Using the Milne transformation, we map the exact scaling solution for a texture as initial condition on our grid, and test for the subsequent evolution. In an empty universe using conformal coordinates, the cosmic scale factor $a = \eta$, so the Milne solution to the Einstein equation in an empty universe becomes

$$ds^2 = -d\tau^2 + \tau^2\left(\frac{dq^2}{1+q^2} + q^2 d\Omega^2\right). \quad (26)$$

With a change of coordinates $r = q\tau$, $t = \tau\sqrt{1+q^2}$ we recover the Minkowski metric $ds^2 = -dt^2 + dr^2 + r^2 d\Omega^2$. Our numerical grid performs very well on this test. Since the same code has very small errors on both limits, we can claim some confidence that it should perform well in between.

IV. RESULTS

A. CBR fluctuations

Using the algorithm outlined in the previous section, we have computed the CBR fluctuations produced by scalar potential fluctuations in an open universe. The results of these calculations are shown in Figs. 3 – 5 for four different observers in $\Omega = 0.21, 0.4$, and $\Omega = 1$ universes. The anisotropy of the grid is visible as an enhancement of the quadrupole in Fig. 5 for $\Omega = 1$. In this case the light rays always move at a constant angle to the grid, so we conclude that even in the worst case, the grid anisotropy has only a minor effect.

In an open universe, the defect dynamics slows down due to the rapid expansion of the universe, which exhibits itself as a loss of power on large angular scales, in particular the quadrupole terms.

The different lines in the figure denote the results from different realizations and the spread in values is a measure of the variance in c_l. The abscissa in the plot is the amplitude of the multipole moments, $c_l = \sum_m a_{lm}^2/(2l+1)$, weighted by $l(l+1)$. In a flat inflationary model with scale-invariant spectrum of fluctuations, $c_l l(l+1)$ is a constant for $l << 200$. Our results imply that for defect models in a low Ω universe, the shape of the multipole spectrum is qualitatively different from other models. The low order multipoles are strongly sup-

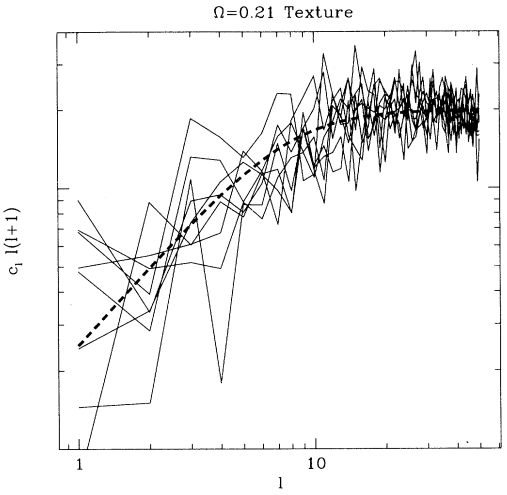

FIG. 3. The eight jagged lines correspond to observers in different universes or at different locations. Flat inflationary models predict $c_l l(l+1)$ as constant. The dashed line is a parametrization of the CBR open universe spectrum: $c_l l(l+1) \propto /[1+(l_{\max}/l)^q]^{1/q}$ with $l_{\max}=8$ and $q=2.5$. In general $l_{\max}$ scales as $\propto \Omega^{-1/2}$.

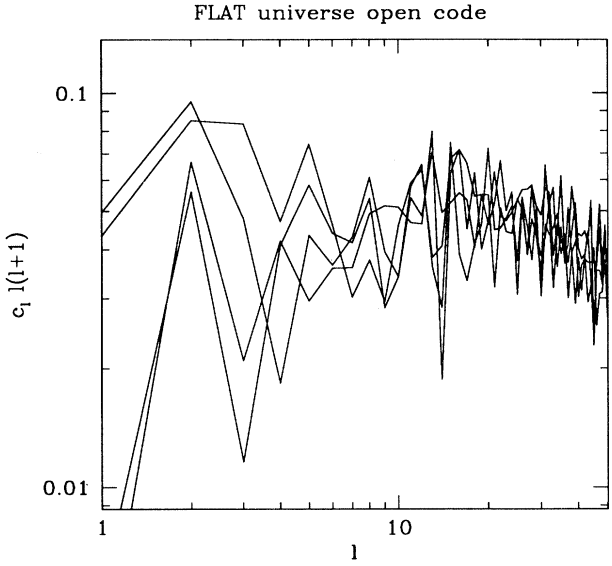

FIG. 5. Nearly flat universe calculated using the open universe code. Here we recover the flat Harrison-Zeldovich spectrum.

pressed, while the multipoles on scales significantly below the angular scale subtended by the curvature scale today still have a scale-invariant form.

For purposes of comparison with the DMR measurements of the temperature fluctuations, we have fitted the results of our numerical simulations with a fitting form

$$c_l l(l+1) = c_0/\left[1+(l_{\max}/l)^{2.5}\right]^{0.4} .$$

The simulations are fit by $l_{\max} \simeq 3\Omega^{0.5}$. Even if the universe is flat, the quadrupole is somewhat suppressed in any model with topological defects as defects on scales comparable to and greater than the horizon size have not yet had time to collapse.

The qualitative features of topological defects in an open universe can be approximated using any flat universe calculation. To first approximation, one can consider the photon sphere we observe today projected back at a redshift of $1+z \approx 1/\Omega$. This will also produce a flat spectrum for large l, with a white noise cutoff for small l. We used our flat space stopped at $z=1$ and $z=1.5$, and the multipole spectrum is depicted in Figs. 6 and 7.

The COBE two-year observations have only been analyzed under the assumption of a power law spectrum of CBR fluctuations [21,22,14]. These analyses conclude that COBE has measured a quadrupole of only 6 ± 3 μK while their fit to larger multipoles imply $Q_{\rm rms} = 20$ μK. In an inflationary model, such a small value for the

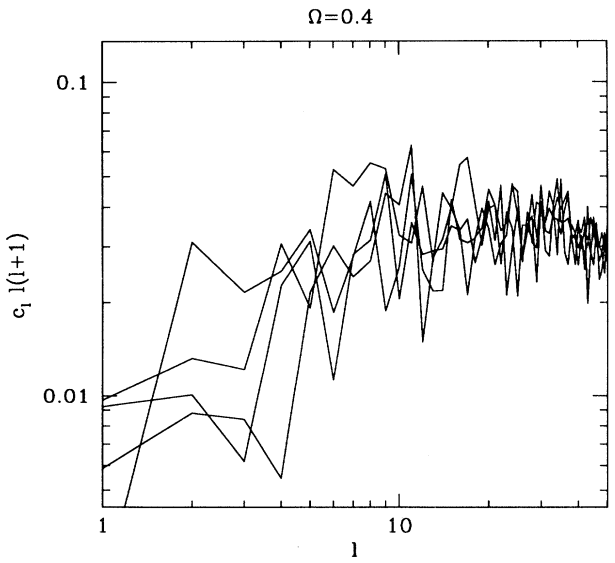

FIG. 4. Same as Fig. 3, but for $\Omega = 0.4$.

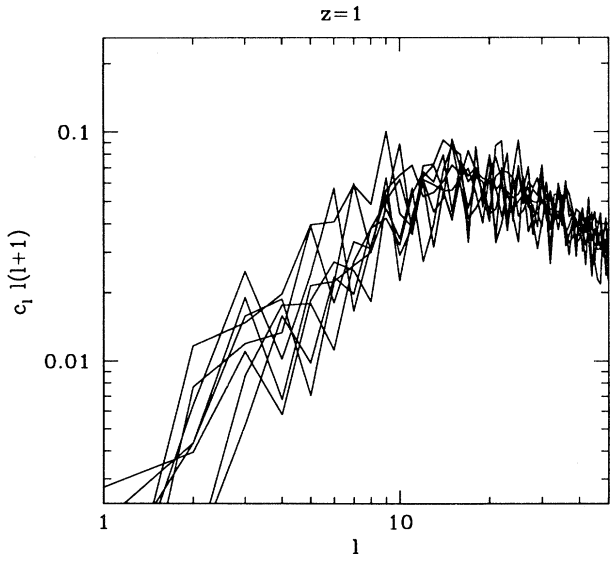

FIG. 6. Flat space simulation at z=1.

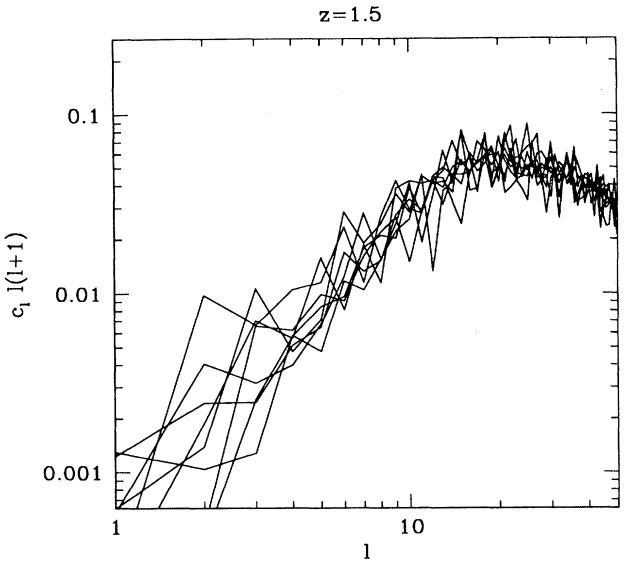

FIG. 7. Flat space simulation at z=1.5.

quadrupole should be observed in less than 5% of the universe. In a defect model in an open universe, the low value for the quadrupole is predicted. On the other hand, COBE two-year measurements do not find a suppression of the $l = 3$ and $l = 4$ modes.

As discussed in Sec. III, our calculations only include the contributions from the scalar growing mode to the CBR fluctuations. The calculations do not include contributions from decaying modes, vector fluctuations, and gravity wave fluctuations. These contributions are subdominant in a flat universe and should be even smaller in an open universe. If these terms were included, then the amplitude of the CBR fluctuations would be increased by a factor $f \sim 1.0 - 1.4$. The upper bound is based on our flat space calculations [7]. Thus, the amplitude of CBR fluctuations needs to be multiplied by this factor.

Topological defect theories have one free parameter: the scale of symmetry breaking, ϕ_0. Note that the abscissas in Figs. 3 – 5 need to be multiplied by $8\pi^2 G\phi_0^2$ to convert the results of the calculations into temperature fluctuations. We will fix this parameter by normalizing our results to the COBE two-year observations by convolving our results with a Gaussian beam with full width half maximum of 10^o and fixing $(\delta T/T)^2_{\rm rms}$ to the value of 40 μK suggested by harmonic analysis of the two-year data [21].

While our calculation did not compute the amplitude of CBR fluctuations on small angular size, we can extrapolate calculation on defects in a flat universe to the open case. Coulson *et al.* [30] found that in a reionized universe, the multipole spectrum was flat from large angular scales to $l \sim 60$. This multipole moment corresponds to the angular size subtended by a texture collapsing near the surface of last scatter in a reionized universe. In an open universe, the relationship between horizon size and angle is altered: $\theta \sim \Omega^{0.5} z^{-0.5}$ for $z \gg \Omega^{-1}$. Thus, we expect that in an open reionized universe, the multipole spectrum would be flat from $l \sim l_{\rm max}$ to $l \sim 60\Omega^{-0.5}$.

If the early universe was not reionized by a generation of star formation before $z \sim 50$, then CBR observations on small angular sizes are probing the universe at $z \sim 1300$, the epoch of recombination. In both defect models and scale-invariant curvature models, there should be a "Doppler peak" at $l \sim 200\Omega^{-0.5}$. In an inflationary model with curvature fluctuations, this peak is produced by the sum of velocity perturbations and the product of potential fluctuations with entropy fluctuations. In these models, the fluctuations are all produced by the growing modes. In a defect model, the "Doppler peak" also has contributions from entropy and potential fluctuations produced by the decaying modes excited by the collapse of defects [29]. As in curvature models, this peak should occur at $l \sim 200\Omega^{-0.5}$, thus measurements of its location may provide a determination of Ω.

Just as in a flat universe, one of the distinctive predictions of a defect model is the non-Gaussian character

TABLE I. Comparison with QDOT observations.

Ω_0	H_0	Required bias		
	(km/s Mpc)	($5h^{-1}$ Mpc)	($10h^{-1}$ Mpc)	($20h^{-1}$ Mpc)
0.2	0.5	3.8–4.7	4.4–5.8	5.3–7.1
0.2	0.6	3.1–3.8	3.6–4.8	4.5–6.1
0.2	0.7	2.6–3.2	3.1–4.1	4.0–5.3
0.2	0.8	2.2–2.8	2.7–3.6	3.6–4.8
0.2	0.9	2.0–2.4	2.4–3.2	3.3–4.4
0.4	0.5	2.8–3.4	3.5–4.6	4.8–6.5
0.4	0.6	2.3–2.8	3.0–4.0	4.3–5.7
0.4	0.7	2.0–2.4	2.6–3.5	3.9–5.2
0.4	0.8	1.7–2.1	2.4–3.1	3.6–4.8
0.4	0.9	1.5–1.9	2.2–2.9	3.4–4.5
1.0	0.5	2.3–2.8	3.4–4.5	5.7–7.6
1.0	0.6	2.0–2.4	3.1–4.0	5.3–7.1
1.0	0.7	1.7–2.2	2.8–3.7	5.0–6.7
1.0	0.8	1.6–2.0	2.6–3.5	4.8–6.5
1.0	0.9	1.5–1.8	2.5–3.3	4.7–6.3

of the temperature fluctuations. This non-Gaussian behavior should be most apparent not in the distribution of temperature fluctuations, but in the distributions of temperature gradients [30,31]. In a flat universe, Coulson *et al.* find that this non-Gaussian character is most apparent on angular size of $\sim 3^o$, the angular size subtended by the surface of last scatter in a reionized universe. In an open Universe, this angular size is shifted to $\sim 3\Omega^{0.5}$ degrees.

While simulations were done only for texture models, the results can easily be extrapolated to other defect models in an open universe. In all of these models, we expect a similar suppression of the low multipoles as the rapid expansion of the Universe slows the evolution of the defects responsible for generating fluctuations on large angular scales.

B. Large-scale structure

Having normalized the defect model to fluctuations in the CBR, we now turn to predictions for mass fluctuations on the scale probed by galaxy surveys. Fluctuations on scales smaller than ~ 1000 Mpc were generated when Ω was close to unity; thus, the results of our earlier work on density fluctuations in a flat universe can be directly extrapolated to open models.

In Pen *et al.* [7], density fluctuation computed by numerical simulations are fit by a function [PST 32,33]

$$P(k) = \frac{D(\Omega)^2}{\Omega h^2} \frac{\alpha k}{[1 + (\beta k) + (\gamma k)^{1.5}]^2} , \qquad (27)$$

where $D(\Omega) \simeq \Omega^{0.7}$ is the ratio of the linear growth to that in an $\Omega = 1$ universe, $\alpha = 225(\epsilon/3.7\times10^{-4})^2/(\Omega h^2)$, $\beta = 3.5/(\Omega h^2)$ Mpc, and $\gamma = 2.75/(\Omega h^2)$ Mpc. Using the normalization in Table I, this directly yields the amplitude of mass fluctuations predicted by linear theory.

On the scale of tens of kiloparsecs, light clearly does not trace mass. This is the source of the missing mass problem. It is less certain whether light traces mass on the scale of several megaparsecs. Cosmologists parametrize this uncertainty by a bias parameter b, the ratio of the variance in the fluctuation in the galaxy counts to the fluctuations in the cosmic density field. Here, we determine the value of b needed to fit astronomical observations.

The Queen Mary, Durnham, Oxford and Toronto (QDOT) survey measured the fluctuations in galaxy counts by obtaining redshifts to a large infrared selected galaxy sample. Saunders *et al.* [32] smoothed their galaxy density field with a Gaussian smoothing window with filter length of $5h^{-1}$, $10h^{-1}$, and $20h^{-1}$ Mpc and found a variance of 0.436 ± 0.091, 0.184 ± 0.05, and 0.0669 ± 0.019 in the density field. The third, fourth, and fifth columns in Table I list the required bias factors needed to fit the central value in the QDOT survey. The statistical uncertainties in the QDOT survey and the COBE measurements lead to a $\sim 25\%$ 1σ uncertainty in b. This is in addition to the uncertainty due to the limitations of our numerical calculations.

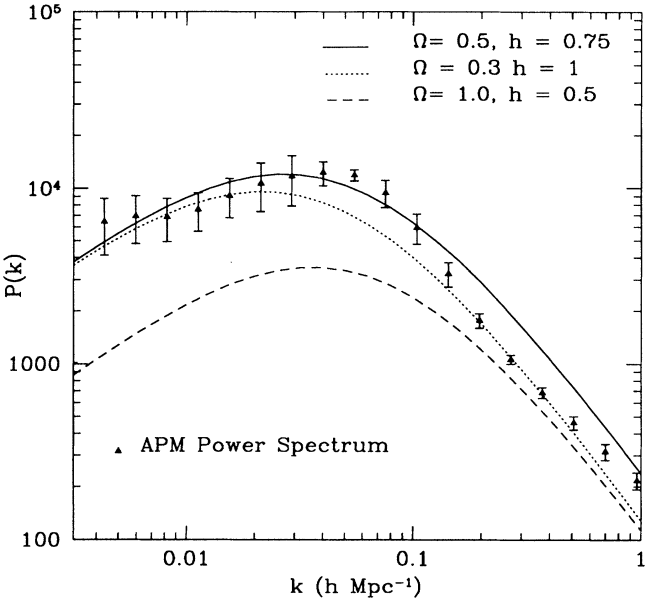

FIG. 8. Comparison of the predicted texture open universe power spectrum to the APM survey for various parameters of Hubble's constant and Ω.

In Fig. 8, we compare the predicted power spectrum of density fluctuations to the power spectrum of galaxy fluctuations inferred from the Automatic Plate Measuring system survey [5]. In this figure, we assumed a bias factor of 1.5.

V. SPECULATIONS

At various points in history, different choices for the curvature of the universe have been considered most natural. Einstein initially considered an eternal and flat universe with a cosmological constant most aesthetically pleasing. But with Hubble's discovery of the universal expansion, the common belief was that the universe should be a closed three sphere, which is bounded in both space and time. This universe would end in a few Hubble times, and thus we would live in a very ordinary epoch. We will use the same Copernican principle to argue that an open universe is almost as well suited.

In the last decade it has become fashionable to return to consider spatially flat universes as most appealing, since there would not be any curvature scale which needs to be explained. This is primarily due to Dicke's anthropic argument, who used the Copernican principle to argue that we should not be living just at the end of the flat epoch. The inflationary paradigm, which appeals to the de Sitter model to solve the "horizon problem," is simplest in a scale-free scenario of a flat universe. But the very problem that they are invented to solve, the absence of a preferred curvature scale, leads to a clash with the Copernican principle as we live at a very special time,

just near the beginning of a matter-dominated universe which would now last for a truly lengthy period of proper time. As we have seen, in the absence of a perfect fluid to label a preferred coordinate frame, the curvature of a universe can be transformed from flat to hyperbolic by a gauge choice. The same holds true for a de Sitter space.

An open universe model does have aesthetic advantages that have been at times overlooked. In an open universe, we are most likely to live in the brief period of time between radiation and curvature domination. Density fluctuations do not collapse during the radiation-dominated epoch and are growing logarithmically slowly during curvature domination. If a universe went directly from a radiation-dominated phase into curvature domination, no structure or life would ever be conceivable. It is only due to a lucky coincidence that we have a slight baryon asymmetry of $\eta = 10^{-11}$, possibly due to baryogenesis in the electroweak phase transition. This allowed structures to form through gravitational instability in the short interval between matter-radiation equality and curvature domination. Since this interval lasts only for a short time, and we live approximately in the center of this period, there is no violation of the Copernican principle. We thus appeal to the observed smallness of electroweak baryogenesis to set the scale for the hyperbolic curvature. Dirac's small number is not really a single small number. The radius of curvature and the horizon size today are simply the product of the proton mass, the baryogenesis photon to baryon ratio, and the smallness of initial fluctuations, observed by COBE to be 10^{-5}, which in the topological defect framework arises from the ratio of the grand unification theory (GUT) scale to the Planck scale. Such a model has no fine tuned parameters.

From a geometric viewpoint, a closed universe is appealing due to its simplicity: a three sphere is the unique universal covering of positively curved three-manifolds, and has a finite volume which would certainly be an attractive property for any designer or process which might have created the universe. But it is interesting to note that there are only a finite number of alternate global topologies which such a designer has to choose from. The projective three-sphere P^3 is one such example. If one analyzes negatively curved spaces, one can of course consider the global covering H^3, but there are many alternatives, including the periodic Poincaré space which we utilized in this paper. The name "open" only applies to the local properties, and we can certainly have a spatially closed "open" universe. If one considers only hyperbolic spaces of finite volume, one finds an infinite number of possible topologies. At fixed curvature R_c, the volumes of these topologies can have collection points on the real line, and one might expect our universe to be chosen from a topology near such a collection point. A number of authors have attempted to calculate transition probabilities between these configurations in 2+1 dimensions [33]. These studies suggest that topological change may well be possible. Unfortunately, as with most quantum gravity calculations, many infinite quantities arise in the process, making it difficult to uniquely predict the outcome of such an estimate.

Whether the negative curvature results from quantum gravitational tunneling, or an alternate exit from the de Sitter phase, or some other yet unknown means, the anthropic principle does set a minimum scale to the curvature radius. In order to bound it from above, one could argue that the intrinsic process forms hyperbolic spacetimes with small curvature, most of which are not observable. So we might live in the smallest allowed scenarios which allow nonlinear structures to form.

However, as we lack a theory of quantum gravity that can predict whether a flat, open, or closed universe is most likely, we believe that all of these models merit careful consideration. Ultimately, this question must be resolved observationally. We have shown that the philosophical arguments that have been invoked to argue for a flat universe are quite ambiguous, and could just as well be used to argue for an open scenario.

VI. CONCLUSIONS

In this paper, we explored the cosmic microwave background signature of defects in an open universe. We have described a new efficient exact solution of the linearized Einstein equations in hyperbolic Friedmann-Robertson-Walker (FRW) spacetimes. The otherwise expensive mode decomposition can be implemented very efficiently thanks to the fast Fourier transform in the Poincaré metric. This formulation was then applied to calculate predictions of texture models in an open universe. We then addressed the classical philosophical arguments including the flatness problem. We showed that the same anthropic and Copernican arguments that were used to argue for a flat universe, are in fact better satisfied in an open model. The curvature scale is naturally explained as a product of three moderately big numbers. The proton mass and the photon-to-baryon ratio set the size of the universe at matter-radiation equality, and the ratio of the GUT to Planck scale that determines expansion factor needed for nonlinear structure to form.

For $\Omega = 0.4$ and $h = 0.7$, the power spectrum of density fluctuations in a COBE-normalized texture model has the correct spectral shape and is consistent with the observed level of galaxy fluctuations for b =2–4. The uncertainty in normalization is a combination of the numerical uncertainties in our calculations and the statistical uncertainties in the observations. A model with $\Omega = 0.4$ and $b = 2$ is consistent with various dynamical measurements of Ω on the scale of clusters and superclusters.

While our work focused on textures in an open universe, we expect qualitatively similar results for other defect models. The basic results appear to be governed by geometry and the changed relationship between angle and physical scale. This is apparent when we compare a flat universe simulation stopped at $1 + z = \Omega^{-1}$ and rescaled by a factor of Ω in angle with an open universe simulation.

Defects in an open universe make a distinctive prediction for the CBR spectrum. In these models, very few fluctuations are generated at late times and at large angular scales. Thus, the models predict a suppression of

the quadrupole and other low multipole moments. The low value of the quadrupole detected by COBE is consistent with this set of theories. A detailed analysis of the COBE DMR results is needed to determine which range of values of Ω are compatible with the observed universe. A qualitative understanding is quite straightforward and is obtained by rescaling the flat space spectra and introducing a break near the curvature scale.

Defects in an open universe are a viable alternative to popular scenarios for structure formation and merit closer study.

ACKNOWLEDGMENTS

We would like to thank Neil Turok for helpful comments. U.P. and D.N.S. were partially supported by NSF Contract Nos. AST 88-58145 and ASC 93-18185 (GC3 HPCC collaboration), NASA Contract No. NAGW-2448, and NSF Grant No. INT91-16745. Numerical calculations were performed on the Convex C3440, which was partially funded by NSF Contract No. AST 90-20863.

APPENDIX A: NOTATION

R_c will denote the curvature radius of the universe, which is given by $R_c = c/(H_0\sqrt{1-\Omega})$. A subscript of 0 denotes a parameter's present value. We use t to denote the proper time, η to measure conformal time. They are related through

$$t = \frac{t_0}{\sinh\eta_0}(\sinh\eta - \eta) \ . \tag{A1}$$

In conformally hyperbolic coordinates, the expansion factor is $a = \cosh\eta - 1 = (2/\Omega) - 2$. The conformal time measures the number of comoving curvature radii traversed by a photon. It is given by $\eta = \cosh^{-1}(2/\Omega - 1)$. We write the FRW metric as

$$ds^2 = -dt^2 + a(t)^2\left(\frac{dr^2}{1+r^2} + r^2 d\Omega^2\right) . \tag{A2}$$

Proper distance between two time-synchronized observers is $\Delta s = aR_c \sinh^{-1} r$. The coordinate r is in units of comoving curvature radii.

APPENDIX B: VACUUM-DOMINATED UNIVERSES

This appendix contains results for a vacuum-dominated flat universe containing dust and vacuum energy. In this universe, the expansion factor can be computed from the energy equation

$$\left(\frac{da}{dt}\right)^2 = H_0^2\left[\Omega_0\frac{a_0}{a} + (1-\Omega_0)\frac{a^2}{a_0}\right] ,$$

where Ω_0, a_0, and H_0 are the density in matter, the expansion factor, and the Hubble constant today and t denotes physical time. This equation can be solved to yield

$$a(t) = \frac{3}{2}\Omega_0^{1/3}(1-\Omega_0)^{1/6}\sinh^{2/3}(H_0 t) \ .$$

The conformal time η in a flat vacuum-dominated universe can be computed with the aid of Gradshteyn and Rhyzik equation (3.166.22):

$$\eta = \int_0^t \frac{dt}{a(t)} = \int_0^a \frac{da}{a(t)(da/dt)} = \int_0^a \frac{dx}{\sqrt{x(1+x^3)}}$$
$$= \frac{1}{3^{1/4}}\mathcal{F}\left[\cos^{-1}\left(\frac{1+(1-\sqrt{3})a}{1+(1+\sqrt{3})a}\right), \frac{\sqrt{2+\sqrt{3}}}{2}\right] \ . \tag{B1}$$

Here, $\mathcal{F}$ is the elliptic integral of the first kind.

It would appear that this complicated relationship between a and η would make it impossible to evaluate Eqs. (6) and (7) analytically. However, by change of variables from η to a, these equations become remarkably tractable:

$$E(a,\tilde{a}) = \int_{\tilde{\eta}}^{\eta}\frac{d\bar{\eta}}{a(\bar{\eta})^2} = \int_{\tilde{a}}^{a}\frac{d\bar{a}}{\bar{a}^2\sqrt{\bar{a}+\bar{a}^4}} = \frac{2}{3}\sqrt{1+a^{-3}}\Big|_{\tilde{a}}^{a} \tag{B2}$$

and

$$H(a,\tilde{a}) = \int_{\tilde{a}}^{a}\frac{d\bar{a}\bar{a}^2}{\sqrt{\bar{a}+\bar{a}^4}}E(\bar{a},\tilde{a})$$
$$= \frac{2}{3}(\bar{a}-a) + \frac{4}{15}\sqrt{1+\bar{a}^{-3}}$$
$$\times\left[\bar{a}_2^{5/6}F_1(\tfrac{1}{2},\tfrac{5}{6};\tfrac{11}{6},-\bar{a})\right]_{\tilde{a}}^{a} \ . \tag{B3}$$

Here, ${}_2F_1$ is Gauss' hypergeometric function. Gradshteyn and Rhyzik equation (3.194.1) was used to compute (B3). Equations (B2) and (B3) can be used to compute CBR fluctuations in a vacuum-dominated model. Note that (B2) and (B3) can also be used to evolve vector and decaying scalar modes:

$$h_i^V(\eta) = 16\pi G\int\Theta_i^V(\tilde{\eta})E(a,\tilde{a})\tilde{a}^2 d\tilde{\eta} \ .$$

APPENDIX C: CLOSED MODELS

In a closed matter-dominated FRW model, the scale factor is

$$a(\eta) = 1 - \cos(\eta) \ . \tag{C1}$$

Thus, the scalar modes are given by Eq. (5) with

$$E(\eta,\tilde{\eta}) = \frac{\dot{a}}{3a}(1+a)\Big|_{\eta}^{\tilde{\eta}} \ ,$$
$$H(\eta,\tilde{\eta}) = \left(\frac{3\bar{\eta}}{2} - 2\sin(\bar{\eta}) + \frac{\cos(\bar{\eta})\sin(\bar{\eta})}{2}\right)\Big|_{\tilde{\eta}}^{\eta}E(\eta,\tilde{\eta}) \ . \tag{C2}$$

The vector modes still satisfy Eq. (13) and with the appropriate form for $a(\eta)$, Eq. (14) describes the evolution of tensor modes.

[1] S.D.M. White, J.F. Navarro, A.E. Evrard, and C.S. Frenk, Nature (London) **366**, 429 (1993).
[2] T.P. Walker, G. Steigman, H. Kang, D.N. Schramm, and K.A. Olive, Astrophys. J. **376**, 51 (1991).
[3] K.B. Fisher, M. Davis, M.A. Strauss, A. Yahil, and J.P. Huchra, Mon. Not. R. Astron. Soc. **267**, 927 (1994).
[4] K.B. Fisher, M. Davis, M.A. Strauss, A. Yahil, and J. Huchra, Mon. Not. R. Astron. Soc. **266**, 50 (1994).
[5] C.M. Baugh and G. Efstathiou, Mon. Not. R. Astron. Soc. **265**, 145 (1993).
[6] A. Albrecht and A. Stebbins, Phys. Rev. Lett. **68**, 2121 (1992).
[7] U. Pen, D.N. Spergel, and N. Turok, Phys. Rev. D **49**, 692 (1994).
[8] R. Durrer and Z. Zhou, Phys. Rev. Lett. **74**, 1701 (1995).
[9] R. Durrer, Fund. Cosmic Phys. **15**, 209 (1994).
[10] J. Borrill, E.J. Copeland, and S. Veeraraghavan, Phys. Rev. D **50**, 2469 (1994).
[11] D.P. Bennett and S.H. Rhie, Astrophys. J. Lett. **406**, L60-E8 (1993).
[12] G.F. Smoot *et al.*, Astrophys. J. **396**, L1 (1992).
[13] E.L. Wright *et al.*, Astrophys. J. Lett. **396**, L13 (1992).
[14] E.L. Wright *et al.*, Astrophys. J. **436**, 443 (1994).
[15] M. Kamionkowski and D.N. Spergel, Astrophys. J. **432**, 1 (1994).
[16] B. Ratra and P.J.E. Peebles, Princeton Report No. PUPT-1444, 1994 (unpublished).
[17] D.N. Spergel, Astrophys. J. Lett. **412**, L5 (1993).
[18] J.R. Bond, R. Crittenden, R.L. Davis, G. Efstathiou, and P.J. Steinhardt, Phys. Rev. Lett. **72**, 13 (1994).
[19] F.C. Adams *et al.*, Phys. Rev. D **47**, 426 (1993).
[20] L.A. Kofman and A.A. Starobinsky, Pis'ma Astron. Zh. **11**, 643 (1985) [Sov. Astron. Lett. **11**, 271 (1985)].
[21] K. Gorski *et al.*, Astrophys. J. **430**, L89 (1994).
[22] C. Bennett *et al.*, Astrophys. J. **436**, 423 (1994).
[23] S. Hancock *et al.*, Nature (London) **367**, 333 (1994).
[24] K. Ganga, E. Cheng, S. Meyer, and L. Page, Astrophys. J. **410**, L57 (1993).
[25] J.R. Gott, Nature (London) **295**, 304 (1982).
[26] R. Durrer, A. Howard, and Z. Zhou, Phys. Rev. D **49**, 682 (1994).
[27] R. Durrer, Phys. Rev. D **42**, 2533 (1990).
[28] N. Turok and D.N. Spergel, Phys. Rev. Lett. **64**, 2736 (1990).
[29] D. Spergel (unpublished).
[30] D. Coulson, P. Ferreira, P. Graham, and N. Turok, Nature (London) **368**, 27 (1994).
[31] R. Moessner, L. Perivolaropoulos, and R. Brandenberger, Astrophys. J. **425**, 365 (1994).
[32] W. Saunders *et al.*, Nature (London) **349**, 32 (1991).
[33] E. Witten, Nucl. Phys. **B323**, 113 (1989).